Control of mutual phase locking of monolithically integrated semiconductor lasers

E. Kapon, J. Katz,[a] C. Lindsey, S. Margalit, and A. Yariv

California Institute of Technology, Pasadena, California 91125

The mutual coherence of two coupled semiconductor lasers is investigated experimentally. It is demonstrated that by varying the gain in the overlap region, the degree of phase coherence can be continuously controlled. The quantitative characterization of the degree of phase coherence by fringe visibility is demonstrated.

Phase-locked laser arrays are a subject of continuing theoretical and practical interest.[1-8] This interest is due mostly to the promise of such arrays to deliver spatially coherent optical beams with power well in excess of that available from single semiconductor lasers.

The major issue in phase-locked laser arrays is the degree of phase locking between the individual laser apertures and its characterization. In this letter we describe a series of experiments in which the mutual coherence of two laser apertures is characterized by measuring the visibility of the far-field interference fringes. We also show, for the first time, how the recently developed[8] separate contact configuration makes it possible to continuously control the degree of coherence.

The separate-contact laser array is depicted in Fig. 1. Separate contacting is accomplished in this device by employing two-level metallization.[8] The 5-μm-wide laser stripes, with 9-μm center-to-center spacing, were delineated by proton bombardment. The lasers were operated under low duty cycle pulsed conditions. Threshold current of each laser, operated alone, was typically 60 mA.

In the first set of experiments described here, we investigated the far-field radiation patterns of pairs of lasers obtained under various conditions. The far-field patterns were displayed on a monitor screen using a silicon-vidicon TV camera. The intensity distribution of the far field, parallel to the junction plane, was obtained by scanning a selected line of the video signal. The corresponding near-field patterns were obtained by imaging the near field using a 20$\times$ objective lens and scanning the pattern in a similar way.

Figure 2 shows the evolution of the near-field and the far-field patterns obtained by operating two lasers 1 and 3 within the array which are separated by 18 μm as the current through laser 2 (between them) was varied. The current through each of the two outermost lasers was kept at the value $I = 1.4I_{th}$. The left and middle columns of Fig. 2 show the near-field and the far-field scans, whereas the right one is a photograph of the far-field pattern taken from the monitor screen. Figure 2(a) shows the patterns obtained when the center laser (2) was unbiased. The far field exhibited interference fringes with an angular spacing of 3°, which resulted from the interference of the two external (1 and 3) laser beams. This angular spacing is in good agreement with the

calculated value of 2.8° (near the center of the pattern). A notable feature of the interference pattern shown in Fig. 2(a) is the low visibility of the fringes. The visibility is defined by[9]

$$v = \frac{(I_{max} - I_{min})}{(I_{max} + I_{min})}, \tag{1}$$

where I_{max} and I_{min} are the intensities at the maximum and the minimum of the fringe pattern, respectively. The visibility of the pattern in Fig. 2(a) (in the center of the pattern) is $v \cong 0.2$. This low visibility is attributed to the weak coupling between the two lasers, which resulted in a low degree of mutual coherence.

Figure 2(b) shows the near-field and the far-field patterns obtained when the center laser (2) was operated *below* threshold (with current $I = 0.2I_{th}$). The interference pattern in the far-field exhibited the same fringe spacing, but the fringe visibility was dramatically increased to $v \cong 0.6$. This higher visibility resulted from the larger coupling between the two lasers caused by the presence of gain in the region between them. The larger gain increased the spread of the optical fields of each laser, towards the region between them,[10] thereby increasing the overlap of these fields. This larger coupling between the two lasers, in turn, resulted in a higher degree of mutual coherence. Indeed, a careful inspection of Fig. 2(b) reveals a slight spread of the near field of each laser.

As the current through the center laser diode was increased the interference pattern underwent further change. In Fig. 2(c), the center laser is operated at $I = 0.5I_{th}$ and in Fig. 2(d), at $I = 0.8I_{th}$. (Note that I_{th} refers to the threshold
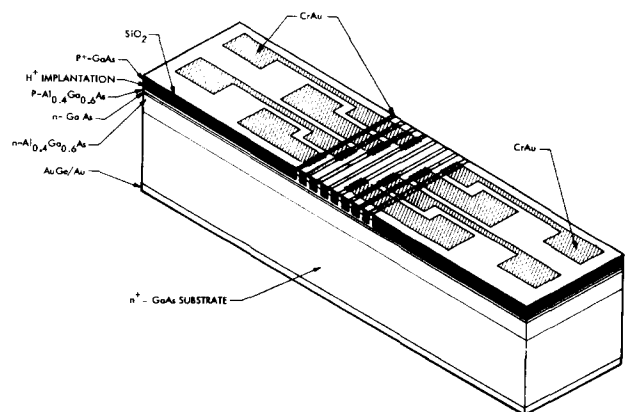

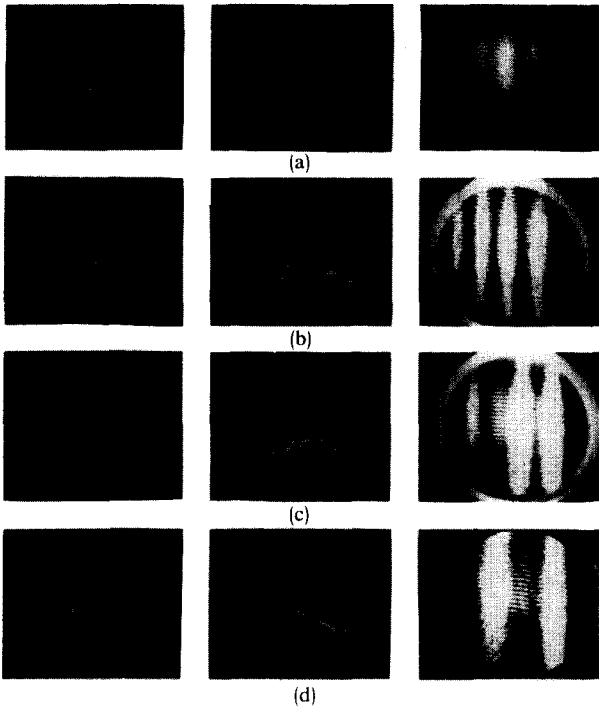FIG. 1. Schematic description of the separate-contact laser array.

FIG. 2. Near-field scans (left column), far-field scans (middle column), and far-field photographs (right column) of two lasers separated by 18 μm, for various currents I_2 through the laser between them. (a) $I_2 = 0$, (b) $I_2 = 0.2I_{th}$, (c) $I_2 = 0.5I_{th}$, (d) $I_2 = 0.8I_{th}$. The horizontal divisions in the far-field scans are at 2.5° separation.

FIG. 3. Far-field scans and photographs for two lasers separated by 45 μm. (a) With no biased lasers between them, (b) with one biased laser at $I = 0.9I_{th}$, (c) with yet another laser biased at $I = 0.1I_{th}$. The horizontal divisions in the far-field scans are at 2.5° separation.

when the laser operates by itself.) Under this latter condition, the near fields of the three lasers have approximately the same peak intensity. The corresponding far field in this case consists of two main lobes separated by 5.8°. The calculated value, for the case of three-slit diffraction grating,[9] is 5.6°. Note the central secondary peak in the far field of Fig. 2(d), which appeared as expected for the diffraction pattern of a three-slit grating. The far field in Fig. 2(c) represents the diffraction pattern for the case of transition between two-slit [Fig. 2(b)] and three-slit [Fig. 2(d)] diffraction patterns.

Figure 3 shows the far field for the case of two-interacting semiconductor lasers separated by 45 μm, that is, with four unbiased lasers between them (see Fig. 1). Figure 3(a) shows the observed far-field pattern when these two lasers are operating simultaneously. The fringes have virtually zero visibility, and the far-field pattern corresponds to the incoherent superposition of the two separate far fields. This indicates that practically no coupling occurred between the two lasers. In Fig. 3(b), we show the effect of operating one of the lasers between these outermost ones below threshold ($I = 0.9I_{th}$). The addition of yet another laser with $I = 0.1I_{th}$ resulted in the pattern shown in Fig. 3(c). The visibility of the fringes increased considerably, to $\nu \cong 0.2$. The angular spacing of the fringes is 1.2°, which agrees well with the calculated value of 1.1°. Once again, the increase in the mutual coherence of the two lasers occurred due to the increase in the coupling between their optical fields in the presence of higher gain in the region between them.

In a second experiment, we investigated the spectrum of two interacting lasers under various degrees of phase locking. The near fields of the two lasers were imaged on the
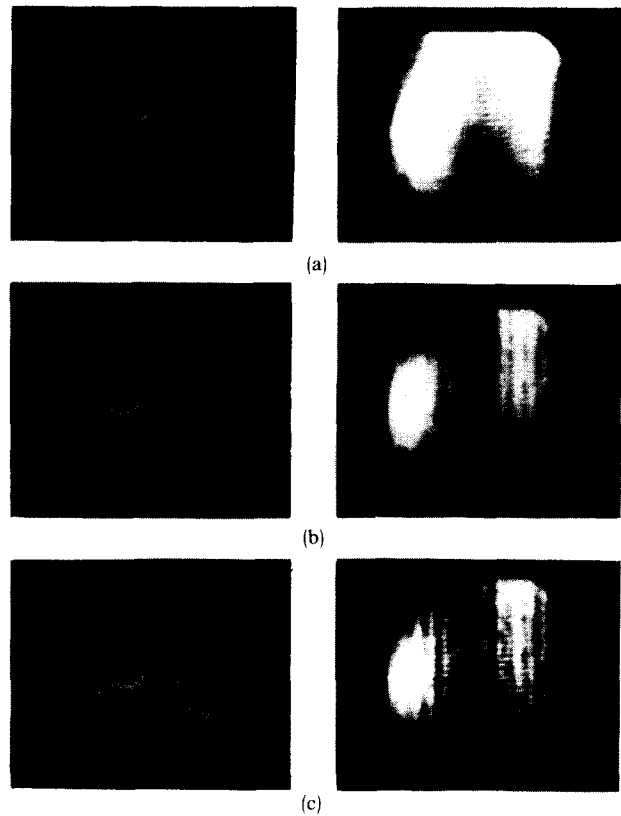
entrance slit of a spectrometer, and their spectrally resolved near fields were displayed on a monitor using a silicon-vidicon TV camera. Figure 4 shows the spectra of two lasers which were separated by 27 μm from each other. In Fig. 4(a), the lasers between them are unbiased, and their observed spectra are not correlated. In Fig. 4(b), we show the effect of introducing gain into the region between these two lasers, by biasing one of the intermediate lasers ($I = 0.4I_{th}$). The modes of the two lasers coalesce into pairs, which is a direct evidence of their phase locking brought about by the increased mode overlap as discussed above.

The results presented in this letter demonstrate the feasibility of controlling the mutual phase locking between semiconductor lasers by varying the gain distribution between their pumped stripes. The results also suggest that the existence of gain below the stripes of a laser array may enhance the coupling between otherwise uncoupled lasers. The observed fringe visibility can evidently be related to the degree of the mutual coherence of the two interacting lasers. It was difficult, however, to derive more quantitative results about the mutual coherence in our experiments, due to the multi-longitudinal mode nature of the lasers and because of their nonidentical intensity distributions. For a given frequency component, it can be shown that

$$\nu = \frac{2\rho^{1/2}}{1 + \rho} \langle \cos \Delta\phi \rangle , \tag{2}$$

where ρ is the ratio of the laser intensities, $\Delta\phi$ their phase difference and $\langle\ \rangle$ indicates time averaging. (It is meant that
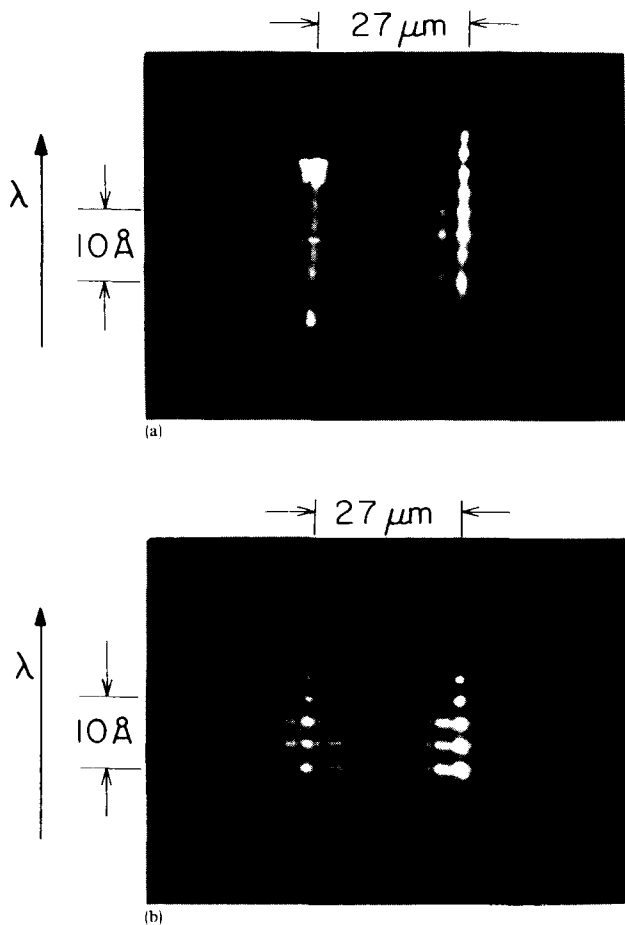
FIG. 4. Spectrally resolved near fields of two lasers separated by 27 μm. (a) Intermediate laser is unbiased, (b) intermediate laser is biased below threshold, $I_2 = 0.4I_{th}$.

$\langle \Delta\phi \rangle = 0$.) It should be noted that the fringe contrast depends weakly on ρ; for example, $\rho = 0.1$ yields $2\rho^{1/2}/(1 + \rho) = 0.57$. Thus, for two single-mode lasers with comparable intensities, a considerable change in the fringe visibility can be attributed mainly to an increase of $\langle \cos \Delta\phi \rangle$. We

should also note that a complete coalescing of the spectra of the coupled lasers was not observed in a similar experiment by Tsang et al.[4] This could be the result of the inherently smaller coupling between the real index guide buried-heterostructure lasers used in their case.

In conclusion, we demonstrated the control of mutual phase locking of semiconductor lasers by variation of the gain distribution between their stripes. The degree of the mutual coherence of the two interacting lasers was observed both in far field and in spectral measurements. This method of control can be employed in laser arrays to obtain controllable phase locking. More quantitative results on the nature of the phase locking would be obtained by carrying out the same experiments described above with an array of single-longitudinal-mode lasers.

[1] D. R. Scifres, R. D. Burnham, and W. Streifer, Appl. Phys. Lett. **33**, 1015 (1978).
[2] D. R. Scifres, W. Streifer, and R. D. Burnham, IEEE J. Quantum Electron. **QE-15**, 917 (1979).
[3] D. R. Scifres, R. D. Burnham, C. Linström, W. Streifer, and T. L. Paoli, Appl. Phys. Lett. **42**, 645 (1983), and references therein.
[4] W. T. Tsang, R. A. Logan, and R. P. Salathe, Appl. Phys. Lett. **34**, 162 (1979).
[5] B. F. Levine, R. A. Logan, W. T. Tsang, C. G. Bethea, and F. R. Merritt, Appl. Phys. Lett. **42**, 339 (1983).
[6] P. E. Ackley and R. W. H. Engelman, Appl. Phys. Lett. **39**, 27 (1981).
[7] J. Katz, S. Margalit, and A. Yariv, Appl. Phys. Lett. **42**, 554 (1983).
[8] J. Katz, E. Kapon, C. Lindsey, S. Margalit, U. Shreter, and A. Yariv, Appl. Phys. Lett. (to be published).
[9] M. Born and E. Wolf, Principles of Optics, 6th ed. (Pergamon, Oxford, 1980).
[10] W. Streifer, R. D. Burnham, and D. R. Scifres, IEEE J. Quantum Electron. **QE-15**, 136 (1979).